The role of triaxiality for the coexistence and evolution of shapes in light krypton isotopes

M. Girod, J.-P. Delaroche
CEA, DAM, DIF, F-91297 Arpajon Cedex, France

A. Görgen, A. Obertelli
CEA-Saclay, IRFU/Service de Physique Nucléaire, F-91191 Gif-sur-Yvette, France

Abstract

The structure of low-lying states in the light krypton isotopes ^{72}Kr, ^{74}Kr, and ^{76}Kr has been studied with the finite-range Gogny D1S effective interaction via Hartree-Fock-Bogolyubov based calculations within a configuration-mixing formalism treating axial and triaxial quadrupole deformations. The good overall agreement with the experimental low-lying excitation spectra and matrix elements supports the shape coexistence scenario and a transition of the ground-state shape from oblate in ^{72}Kr to prolate in ^{76}Kr. The triaxial degree of freedom is shown to be crucial to reproduce the experimental data in general and the inversion of the oblate and prolate configurations in particular.

Key words:
PACS: 21.60.Jz, 21.10.Re, 21.10.Ky, 27.50.+e

Most atomic nuclei are deformed in their ground state, while spherical symmetry is usually only realized in nuclei with closed proton or neutron shells. Microscopically, nuclear deformation occurs if there are sufficiently large energy gaps (compared to the pair scatter energy) between the nucleon orbitals at finite values of deformation. The stabilizing effect of deformed shell gaps causes minima in the potential energy surface (PES) at non-spherical shapes. The deformation can be expressed in a multipole expansion of the matter distribution or, alternatively, of the charge distribution, which is more easily accessible experimentally. Quadrupole shapes are by far the most important type of deformation and are conveniently described by the parameters β and γ for the axial deformation and the deviation from axiality, respectively [1]. The features of most deformed nuclei are consistent with an axially symmetric, elongated (prolate) shape. Flattened (oblate) shapes are less common, and only few nuclei are expected to be oblate in their ground state [2,3].

The same nucleus can assume different shapes, which can change dramatically with angular momentum and excitation energy, for example when a deformed configuration becomes favored due to its large moment of inertia. The energies of the different configurations also change with proton or neutron number, so that the nuclear shape, for example for the ground state, can change from one nuclide to another. Such shape transitions involving coexisting configurations of different shapes have to be distinguished from shape changes due to an evolving mean-field potential, *e.g.* from spherical to deformed, as was already pointed out by Heyde *et al.* [4].

We define shape coexistence as the existence of states of the same spin and parity corresponding to different shapes within the same nucleus. This is very common, as different configurations of the nucleons, occupying different orbitals, will generally lead to different equilibrium shapes. Nevertheless, the shapes will be rather similar in most cases. We therefore speak of shape coexistence in the proper sense only if (i) the shapes involved are clearly distinguishable, *e.g.* spherical vs. deformed or prolate vs. oblate, and if (ii) the energies of the states are similar, but separated by a barrier, so that mixing between the different components of the wave functions is weak and the states retain their character. This can occur if two distinct minima with similar absolute energy coexist in the PES. Shape coexistence has been predicted theoretically and observed experimentally in several regions of the nuclear chart [5]. Since the nuclear deformation is in general very sensitive to the nuclear structure, shape coexistence represents a particularly stringent test for nuclear structure theory. In this letter we demonstrate the importance of triaxiality for the coexistence of prolate and oblate shapes and their evolution with neutron number in the light krypton isotopes.

Prolate and oblate configurations are competing to form the ground state in the isotopes ^{72}Kr, ^{74}Kr, and ^{76}Kr. Shape coexistence was first suggested to explain the irregularities in the ground-state bands [6,7] and the origin of the low-lying 0_2^+ states in these nuclei [8,9]. The systematics of the excitation energy of the 0_2^+ states and their electric monopole transition strength to the ground state was interpreted as an indication for a transition from a prolate ground-state shape in ^{76}Kr to oblate in ^{72}Kr, with strongly mixed configurations for ^{74}Kr [9]. The latter is supported by the comparison of the Gamow-Teller strength distribution in the β decay of ^{74}Kr with deformed Quasiparticle-Random-Phase-Approximation calculations, suggesting a strong prolate-oblate shape coexistence in the ground state of ^{74}Kr [10]. Recent results from low-energy Coulomb excitation of ^{74}Kr and ^{76}Kr provide the sign of the electric quadrupole moments for several low-lying states in these nuclei, proving the prolate character of the states in the ground-state band and oblate shapes for an excited configuration [11]. Finally, the transition probability $B(E2; 0_1^+ \to 2_1^+)$ in ^{72}Kr has been determined by Coulomb excitation at intermediate energy [12]. Comparing the relatively small value to theoretical calculations, this result has been interpreted as supporting an oblate ground state in ^{72}Kr.

Several theoretical approaches, such as shell-model methods [13,14], self-consistent triaxial

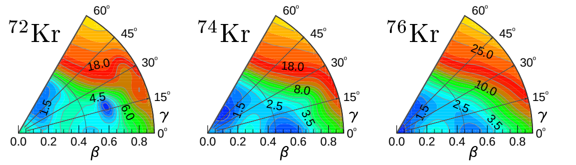

Fig. 1. Potential energy surfaces for ^{72}Kr, ^{74}Kr, and ^{76}Kr.

mean-field models [15,16], or beyond-mean-field models [17], predict shape coexistence at low excitation energy in the light krypton isotopes. However, the transition from a prolate ground-state shape in ^{76}Kr and ^{74}Kr to oblate in ^{72}Kr has only been reproduced in the so-called excited VAMPIR approach, which uses a valence space reduced to the *fpg* shells and a modified G matrix with effective charges [14]. This approach has only limited predictive power since the shell-model interaction is locally derived for a given mass region. On the other hand, no self-consistent mean-field (and beyond) calculation with a globally derived interaction has reproduced this feature of the light krypton isotopes so far. A beyond-mean-field study of the low-lying states and their configuration mixing in the light Kr isotopes with the Skyrme interaction SLy6, restricted to axial symmetry, found oblate ground-state shapes coexisting with excited prolate configurations for all light Kr isotopes [17] [1].

In this letter we present Hartree-Fock-Bogolyubov (HFB) based configuration-mixing calculations using the Generator Coordinate Method (GCM) with Gaussian Overlap Approximation (GOA) for the low-lying states in ^{72}Kr, ^{74}Kr, and ^{76}Kr with the finite-range, density-dependent Gogny D1S effective interaction [19,20] including axial and triaxial quadrupole deformations and the rotational degrees of freedom with no free parameters. It has already been shown that such calculations reproduce the experimental excitation energies and $B(E2)$ transition strengths in this region of the nuclear chart well [11,21]. Here we describe the calculations in more detail and show that the five-dimensional nature of the calculations is essential for the correct description of the complex shape coexistence, and that triaxial shapes play a crucial role for the transition from oblate ground-state shape in ^{72}Kr to prolate in ^{76}Kr.

In the present GCM+GOA approach, the correlated states are described as a superposition of the

[1] This beyond-mean-field method based on Skyrme interactions has recently been extended to triaxial degree of freedom [18].

quasiparticle vacuum wave functions $|\phi_q\rangle$ which are obtained from the minimization of the energy functional

$$\delta\langle\phi_q|\hat{H} - \sum_i \lambda_i \hat{Q}_i - \lambda_Z \hat{Z} - \lambda_N \hat{N}|\phi_q\rangle = 0\,, \tag{1}$$

where $\hat{H}$ is the nuclear many-body Hamiltonian built with the finite-range effective force D1S [20], $\hat{Q}_i$ is the set of external field operators, and $\hat{Z}$ and $\hat{N}$ are the proton and neutron number operators, respectively. The Lagrange multipliers λ_i, λ_Z, and λ_N are determined by the constraints

$$\langle\phi_q|\hat{Q}_i|\phi_q\rangle = q_i\,,\ \langle\phi_q|\hat{Z}(\mathrm{or}\hat{N})|\phi_q\rangle = Z(\mathrm{or}N)\,. \tag{2}$$

The correlated states write

$$|\Psi_k\rangle = \int f_k(q)|\phi_q\rangle\, dq\,, \tag{3}$$

where q stands for a set of collective coordinates and where the superposition amplitude $f_k(q)$ is the solution of the Griffin-Hill-Wheeler equation [22,23]. This integral equation is transformed via the GOA into a second-order differential equation, which writes in the laboratory system of coordinates [24]

$$\hat{\mathcal{H}} g_k(q) = E_k g_k(q)\,, \tag{4}$$

with

$$\hat{\mathcal{H}} = -\frac{\hbar^2}{2}\sum_{ij}\frac{\partial}{\partial q_i}\left[M^{-1}(q)\right]_{ij}\frac{\partial}{\partial q_j} + \mathcal{V}(q)\,. \tag{5}$$

In the present work, the operator $\hat{\mathcal{H}}$ is a microscopic collective Hamiltonian relevant to the five quadrupole coordinates, *i.e.* axial q_0 and triaxial q_2 deformation as well as the three Euler angles, $g_k(q)$ is the Gauss transform of the amplitude $f_k(q)$, M_{ij} the tensor of inertia, and $\mathcal{V}(q)$ the PES corrected for the zero-point energy

$$\mathcal{V}(q) = \langle\phi_q|\hat{H}|\phi_q\rangle - \Delta V(q),\ q = (q_0, q_2)\,. \tag{6}$$

The zero-point energy correction $\Delta V(q)$ includes rotational and vibrational components [25]. The collective masses B_{ij} entering the tensor of inertia are calculated in the cranking approximation [26,27]. In contrast, the moments of inertia $\mathcal{J}_i(q)(i = 1, 2, 3)$ are calculated self-consistently at spin zero [28,29]. Changes of collective masses or moments of inertia with the rotational frequency of the nucleus are not considered in this approach, reducing the predictive power of the model to low spins only.

The Schrödinger-like Eq. (4) has eigenstates which may be expressed as

$$|IM\rangle = \sum_{K=0}^{I} g_K^I(\beta,\gamma)\,|IMK\rangle\,, \tag{7}$$

where the deformation parameters β and γ are related to the coordinates q_0 and q_2 [24], $|IMK\rangle$ is a linear combination of Wigner rotation matrices with M and K being projections of the angular momentum I onto the third axis in the laboratory and inertia frame, respectively, and $g_K^I(\beta,\gamma)$ is interpreted as vibration amplitude. It follows that the probability density $\rho^I(\beta,\gamma)$ of a state with angular momentum I in the (β,γ) plane is

$$\rho^I(\beta,\gamma) = \sum_{K=0}^{I}\left|g_K^I(\beta,\gamma)\right|^2 \mu(\beta,\gamma)\,, \tag{8}$$

where $\mu(\beta,\gamma)$ is the metric of the Hamiltonian $\hat{\mathcal{H}}$ [24,30]. By construction, $\rho^I(\beta,\gamma)$ is normalized over the sextant $S_I = \{\beta \geq 0,\ 0° \leq \gamma \leq 60°\}$.

The PESs $\mathcal{V}(q)$ are shown in Fig. 1. Two distinct minima of almost equal depth are observed for all three Kr isotopes under study, separated by a triaxial barrier of approximately 2 MeV. For ^{74}Kr and ^{76}Kr the minima are found at axial shapes with large prolate $(\beta = 0.5, \gamma = 0°)$ and smaller oblate deformation $(\beta = 0.2, \gamma = 60°)$. For ^{72}Kr the absolute minimum is found at oblate deformation, while the prolate minimum has moved to a triaxial shape with $\gamma \approx 15°$, giving already a first hint of the importance of triaxial shapes for the description of low-lying states in the Kr isotopes. Note, however, that the location of a minimum in the PES does not yet determine the nuclear shape, as correlations beyond the mean field have to be taken into account.

The excitation energies and quadrupole moments of the low-lying states in ^{72}Kr, ^{74}Kr, and ^{76}Kr and the transition probabilities between them were obtained from the calculations after configuration mixing following the method of Kumar [31]. Detailed experimental data are available for ^{74}Kr and ^{76}Kr, and the excellent agreement with our calculations has already been demonstrated in Ref. [11]. Experimental information on ^{72}Kr, however, is sparse. A comparison between experimentally known data and our calculation is shown in Fig. 2. The only known transition probability is $B(E2; 2_1^+ \rightarrow 0_1^+) = 1000 \pm 130$ e^2fm^4 [12]. The calculated excitation energies are higher than the experimental values, in particular for the 0_2^+ state. On the other hand, also the exper-

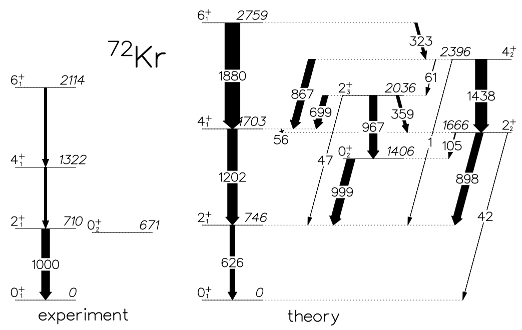

Fig. 2. Experimental and calculated excitation spectrum of low-lying states for ^{72}Kr. The spin-parity and excitation energy (in keV) is indicated for each state. The width of the arrows is proportional to the reduced transition probability $B(E2)$, which is given in e^2fm^4.

imental excitation spectrum is stretched compared to ^{74}Kr and ^{76}Kr, so that the systematic trend is correctly reproduced by the calculations. The transition strength in the ground-state band is found to increase with spin in all three isotopes, which is due to the strong configuration mixing in the low-spin states. The calculated energies of the 0_2^+ states and some selected B(E2) values, which are revealing for the shape coexistence, are compared to experimental values in Table 1. The calculations overestimate the excitation energies of the 0_2^+ states in all three isotopes, but the systematic trend is again correctly reproduced with a minimum in ^{74}Kr. At the same time, the coupling between the 0_2^+ and the 2_1^+ states, which is strong for all isotopes under study, has a maximum for ^{74}Kr. This supports the interpretation of ^{74}Kr showing the strongest configuration mixing.

Further information on the degree of shape mixing can be derived from an evaluation of the electric monopole strength $\rho^2(E0; 0_2^+ \to 0_1^+)$, which was calculated as

$$\rho^2(E0; 0_2^+ \to 0_1^+) = |\frac{\langle 0_2^+ | \sum_{i=0}^{Z} r_i^2 | 0_1^+ \rangle}{R^2}|^2, \tag{9}$$

with $R = 1.2A^{1/3}$ fm. The results are shown in Fig. 3 together with experimental measurements [8,9,32] and calculations based on mixing of axial mean-field configurations using the SLy6 effective force [17]. Even though the absolute values found in our (parameter-free) calculations are too large by an almost constant factor of three, the systematic trend is well reproduced. The increase of the $\rho^2(E0)$ value from ^{78}Kr to ^{74}Kr indicates increased configuration mixing, which is found lower again for ^{72}Kr. These results are consistent with a maximum configuration mixing in ^{74}Kr and an inversion of the ground-state shape for ^{72}Kr. While the absolute values from the axial GCM calculations [17] are in better agreement

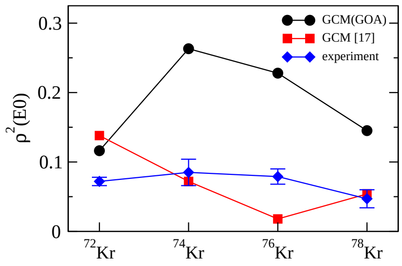

Fig. 3. Electric monopole matrix elements $\rho^2(E0)$ for the chain of light Kr isotopes in comparison with results from the axial Skyrme GCM calculation [17] and experimental values [8,9,32].

with experiment, they do not reproduce the systematic trend, consistent with the fact that they do not find an inversion of prolate and oblate shapes.

The nature of the low-lying states and their associated shapes can be understood by examining the topology of the collective wave functions. The probability densities $\rho^I(\beta,\gamma)$ (Eq. 8) for the states in the ground-state bands of ^{72}Kr, ^{74}Kr, and ^{76}Kr are shown in Fig. 4. The spectroscopic quadrupole moment Q_s (in the laboratory frame) and the relative weight of $K = 2$ components are also given. Prolate (oblate) states with predominant $K = 0$ components have negative (positive) Q_s moments. Note, however, that in our calculation K is always evaluated with respect to the prolate axis, so that states of axially symmetric oblate shapes have $K \neq 0$, and a transformation of the spectroscopic quadrupole moment into the intrinsic frame of reference with this definition of K is not straight forward. States with $I^\pi = 0^+$ have $K = 0$ and $Q_s = 0$ by definition. It should be noted that $\rho^I(\beta,\gamma) = 0$ at $\gamma = 0°$ and $60°$ due to the metric of the Hamiltonian [24]. The spectroscopic quadrupole moments, which are known experimentally (including their sign) for several states in ^{74}Kr and ^{76}Kr, are in rather good agreement with our calculations, as was already discussed in Ref. [11].

The ground-state wave function is strongly spread out for all three isotopes. The 2_1^+ states show a shape transition from prolate in ^{76}Kr to oblate in ^{72}Kr, with ^{74}Kr showing shape coexistence with a dominating prolate and a smaller oblate component of the wave function. This is also reflected in the sign of the quadrupole moment Q_s, which is negative for the 2_1^+ states in ^{76}Kr and ^{74}Kr, but positive for ^{72}Kr. The probability densities for the 4_1^+ states are much more localized at prolate shape in the case of ^{76}Kr and ^{74}Kr, whereas the 4_1^+ state in ^{72}Kr shows shape coexistence with two distinct prolate and oblate components. The 6_1^+ states have prolate character in all three isotopes. The topology of

Table 1
Comparison of calculated and experimental excitation energies of the 0_2^+ states (in keV) [9,6], $B(E2)$ values involving both 0_1^+ and 0_2^+ states (in e^2b^2) [11,12], $\rho^2(E0; 0_2^+ \to 0_1^+)$ values [8,9,32], and charge radii (in fm) [34].

		^{72}Kr	^{74}Kr	^{76}Kr
$E(0_2^+)$	ex.	671	508	770
	th.	1406	748	926
$B(E2; 2_1^+ \to 0_1^+)$	ex.	0.100(13)	0.122(2)	0.144(2)
	th.	0.063	0.104	0.117
$B(E2; 0_2^+ \to 2_1^+)$	ex.	—	0.47(5)	0.241(11)
	th.	0.100	0.364	0.234
$\rho^2(E0)$	ex.	0.072(6)	0.085(19)	0.079(11)
	th.	0.116	0.263	0.228
R_c	ex.	4.164(7)	4.187(4)	4.202(3)
	th.	4.145	4.179	4.198

the wave functions indicates hence a transition of the ground-state shape with neutron number from prolate in ^{76}Kr to oblate in ^{72}Kr, as well as a shape transition with angular momentum for ^{72}Kr from oblate at the ground state to prolate above $I \geq 6$. The terms *prolate* and *oblate*, however, should be used with caution, because for some cases the probability densities extend strongly into the triaxial plane, and the $K = 2$ contribution is large. This is in particular true for the non-yrast states, for which the probability densities are generally more complex and characterized both by coexistence of prolate and oblate shapes and by mixing of $K = 0$ and $K = 2$ components. The transition from a prolate to an oblate state (or vice versa) is thus understood as a transition via non-axial shapes, rather than along the axial path. A similar result was found in calculations for ^{72}Kr using the method of self-consistent adiabatic large-amplitude collective motion [33].

The shape transition with neutron number is also reflected in the mean-square charge radii for the ground states. An increase in the charge radius is observed experimentally from $N = 50$ to $N = 40$ [34], reflecting increasing deformation, but the radius drops sharply from ^{76}Kr to ^{72}Kr, consistent with a shape transition from prolate to oblate. The good agreement between experimental [34] and calculated charge radii is illustrated in Table 1. It is also consistent in this context that the axial GCM calculations with Skyrme force by Bender *et al.*, which find oblate ground states for all light Kr isotopes, do not reproduce the isotopic shift of the charge radii [17].

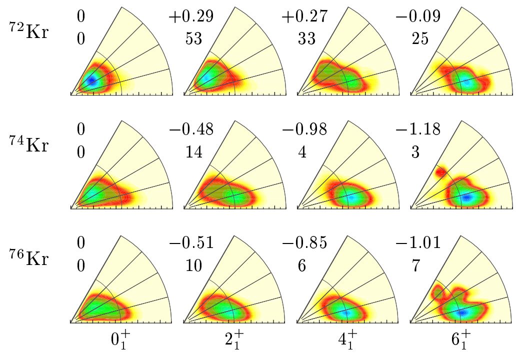

Fig. 4. Probability density $\rho^I(\beta,\gamma)$ for the collective wave functions of the states in the ground-state bands of ^{72}Kr, ^{74}Kr, and ^{76}Kr. The scale for the deformation parameters is the same as for the potential energy surfaces in Fig. 1. The values shown for each state give the spectroscopic quadrupole moment Q_s (eb) and the relative weight of $K = 2$ components (in %) (see text).

The analysis of both the probability density of the wave functions and of the mean-square charge radii confirms the shape coexistence scenario in the light krypton isotopes, with the oblate configuration energetically lowest in ^{72}Kr and the prolate configuration favored in ^{74}Kr and ^{76}Kr. A similar shape transition is found in the light Se isotopes with an oblate configuration dominating the ground state in the $N = Z$ isotope ^{68}Se and a coexisting prolate configuration, whose energy is decreasing with neutron number [21]. As in the case of ^{72}Kr, the oblate shapes found in the Se isotopes turn prolate with increasing angular momentum, with the critical spin for this shape transition depending on the relative energies of the oblate and prolate configurations [21].

To further investigate the role of triaxiality for the shape transition in the light krypton isotopes, calculations were performed for the 0^+ states in the three Kr isotopes using the same approach restricted to axial shapes. Only the axial quadrupole moment q_0, here taken along the z-axis, was considered as collective coordinate, which takes on negative and positive values, thus covering both oblate ($q_0 < 0$) and prolate ($q_0 > 0$) intrinsic shapes. A collective Hamiltonian in one dimension - spanned by q_0 - is then defined. The potential energy $\nu(q_0)$ is found as

$$\nu(q_0) = \langle \Phi_{q_0} | \hat{H} | \Phi_{q_0} \rangle - \Delta V(q_0), \qquad (10)$$

where $\Delta V(q_0)$ is a short notation for the zero-point energy correction including (i) the same rotational component as previously, and (ii) the vibrational component associated with q_0. Also the collective mass is only associated with the q_0 coordinate. Solving the Hamiltonian in one dimension leads to eigenstates characterized by I=K=0. The first and second

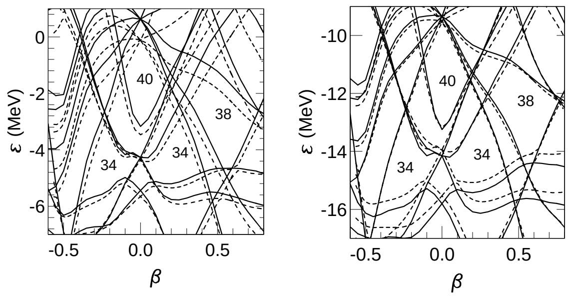

Fig. 5. Nilsson diagrams for protons (left) and neutrons (right) for ^{74}Kr obtained in the Gogny D1S (full lines) and Skyrme SLy6 (dashed lines) calculations [35]. The quadrupole deformation β is proportional to the axial quadrupole moment q_0.

eigenstates are interpreted as ground and 0_2^+ state, respectively. The results still indicate shape coexistence. However, the ground states were found to be dominated by oblate shapes for all three Kr isotopes under study, contrary to experimental results [11]. The average charge quadrupole deformation $\langle q_0 \rangle$ for the ground states in ^{72}Kr, ^{74}Kr, and ^{76}Kr is found to be -308, -203, and -58 $e$fm^2, respectively. The equivalent values from the axial Skyrme calculations of Bender *et al.* are similar: -302, -124, and -154 $e$fm^2 [17,35]. In the latter work this deficiency was attributed to an incorrect description of the single-particle energies in the *fp* shell by the SLy effective interactions. Our results, however, show that the restriction to axial shapes is responsible for favoring the oblate configuration. In fact, the single-particle energies obtained with the SLy6 and D1S interactions are very similar, as illustrated in Fig. 5, showing the consistency of the two calculations on the mean-field level. It may then be concluded that triaxiality plays a key role for explaining shape transitions in the light Kr isotopes.

In summary, we have performed HFB-based configuration-mixing calculations with the finite-range Gogny D1S interaction for the light krypton isotopes, treating all quadrupole deformations in a formalism using a Bohr-like Hamiltonian. Good agreement is found with experimental excitation energies, transition probabilities, quadrupole moments, and charge radii. The structure of the low-lying states is dominated by the coexistence of prolate and oblate shapes, which change rapidly from one state to another, making the assignment of band structures difficult. Even though differences related to the choice of the effective interaction cannot be excluded entirely, our results suggest that it is essential to include non-axial shapes in GCM calculations in order to correctly describe the shape coexistence and shape transitions in the light Kr isotopes. This question will be ultimately settled once triaxial GCM calculations along the lines of Ref. [18], both with Skyrme and Gogny interactions, will become feasible in this mass region.

The authors would like to thank M. Bender for enlightening discussions and providing unpublished data.

References

[1] A. Bohr and B.R. Mottelson, *Nuclear Structure* (W.A. Benjamin, Reading 1975).
[2] N.J. Stone, At. Data Nucl. Data Tables 90 (2005) 75.
[3] N. Tajima, N. Suzuki, Phys. Rev. C 64 (2001) 037301.
[4] K. Heyde *et al.*, Phys. Rev. C 69 (2004) 054304.
[5] J.L. Wood *et al.*, Phys. Rep. 215 (1992) 101.
[6] R.B. Piercey *et al.*, Phys. Rev. Lett. 47 (1981) 1514.
[7] B.J. Varley *et al.*, Phys. Lett. B 194 (1987) 463.
[8] C. Chandler *et al.*, Phys. Rev. C 56 (1997) R2924.
[9] E. Bouchez *et al.*, Phys. Rev. Lett. 90 (2003) 082502.
[10] E. Poirier *et al.*, Phys. Rev. C 69 (2004) 034307.
[11] E. Clément *et al.*, Phys. Rev. C 75 (2007) 054313.
[12] A. Gade *et al.*, Phys. Rev. Lett. 95 (2005) 022502; Phys. Rev. Lett. 96 (2006) 189901(E).
[13] K. Langanke, D.J. Dean, and W. Nazarewicz, Nucl. Phys. A 728 (2003) 109.
[14] A. Petrovici, K.W. Schmid, A. Faessler, Nucl. Phys. A 665 (2000) 333.
[15] P. Bonche *et al.*, Nucl. Phys. A 443 (1985) 39.
[16] M. Yamagami, K. Matsuyanagi, and M. Matsuo, Nucl. Phys. A 693 (2001) 579.
[17] M. Bender, P. Bonche, and P.H. Heenen, Phys. Rev. C 74 (2006) 024312.
[18] M. Bender, P.H. Heenen, Phys. Rev. C 78 (2008) 024309.
[19] J. Dechargé, D. Gogny, Phys. Rev. C 21 (1980) 1568.
[20] J.-F. Berger, M. Girod, and D. Gogny, Comput. Phys. Commun. 63 (1991) 365.
[21] J. Ljungvall *et al.*, Phys. Rev. Lett. 100 (2008) 102502.
[22] D.L. Hill and J.A. Wheeler, Phys. Rev. 89 (1953) 1102.
[23] J.J. Griffin, J.A. Wheeler, Phys. Rev. 108 (1957) 311.
[24] J. Libert, M. Girod, and J.-P. Delaroche, Phys. Rev. C 60 (1999) 054301.
[25] M. Girod, B. Grammaticos, Nucl. Phys. A 330 (1979) 40.
[26] D.R. Inglis, Phys. Rev. 103 (1956) 1786.
[27] S.T. Belyaev, Nucl. Phys. A 24 (1961) 322.
[28] D.J. Thouless, J.G. Valatin, Nucl. Phys. A 31 (1962) 211.
[29] M. Girod *et al.*, Phys. Lett. B 325 (1994) 1.
[30] K. Kumar, M. Baranger, Nucl. Phys. A 92 (1967) 608.
[31] K. Kumar, in *The Electromagnetic Interaction in Nuclear Spectroscopy*, Ed. W.D. Hamilton (North-Holland, Amsterdam,1975), p.89.
[32] A. Giannatiempo *et al.*, Phys. Rev. C 52 (1995) 2444.
[33] D. Almehed, N.R. Walet, Phys. Lett. B 604 (2004) 163.
[34] I. Angeli, At. Data Nucl. Data Tables 87 (2004) 185.
[35] M. Bender, private communication.